The visualization of 3D stress and strain tensor fields

Burkhard Wünsche
Department of Computer Science, University of Auckland,
Private Bag 92019, Auckland, New Zealand
email: burkhard@cs.auckland.ac.nz

ABSTRACT

Second-order tensors are a fundamental entity in engineering, physical sciences and biomechanics. Examples are stresses and strains in solids and velocity gradients in fluid flows. The visualization of tensor fields improves the understanding and interpretation of tensor data and is therefore of paramount importance for the scientist. This paper gives an introduction to the definition and visualization of stress and strain tensor fields suitable for the Computer Scientist. Several visualization methods for tensor fields are introduced with a simple example.

1 Introduction

During the past few years, physically based modelling has emerged as an important new approach to computer animation and computer graphics. An important subfield is the modelling of elastic bodies, which among others are used in computer animation [5] and surgical simulation [6]. A mathematical description of elastic bodies is given by the theory of *elasticity*, which is the study of the deformation of a solid body under loading together with the resulting stresses and strains.

Stresses and strains are important since they are related to material deformation and material failure. Unfortunately stresses and strains are tensors having the same complexity as matrices. Large amounts of tensor data are hence difficult to interpret. The visualization of tensor fields improves the understanding and interpretation of tensor data and is therefore of paramount importance in the fields of engineering, medicine, and biomechanics.

In this paper we give an introduction to the definition and visualization of stresses and strains suitable for the Computer Scientist without an engineering background.

2 Notations and Definitions

For simplicity we use a rectangular Cartesian coordinate system with the base vectors $\mathbf{e}_1$, $\mathbf{e}_2$, and $\mathbf{e}_3$. Vectors are written in small bold Latin letters and tensors in capital bold Latin letters or small bold Greek letters. We only deal with second-order tensors which are linear transformations between vectors and can be represented by matrices.

An important property of an n-dimensional symmetric tensor $\mathbf{T}$ is that there are

always n *eigenvalues* λ_i and n mutually perpendicular *eigenvectors* $\mathbf{v}_i$ such that

$$\mathbf{T}\mathbf{v}_i = \lambda_i \mathbf{v}_i \quad i = 1, \ldots, n \tag{1}$$

3 Displacement and Strain

An elastic body under an applied load deforms into a new shape. We want to find a mathematical description for the displacement the body undergoes. For a one-dimensional example consider a thin rubberband as pictured in figure 1. Two arbitrary points P and Q are marked at position x and $x + \delta x$, respectively. After deformation these points move to position $x + u$ and $x + u + \delta x + \delta u$, respectively, where u is called the *displacement*. The total length increase between these points is δu. The *strain* is now defined as the increase per unit length, i.e., the displacement gradient, which in one dimension is defined as

$$\epsilon_x = \lim_{\delta x \to 0} \frac{\delta u}{\delta x} = \frac{du}{dx}$$

In higher dimensions the situation is more complicated. Figure 2 shows a body

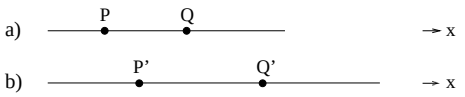

Figure 1: A rubberband before (a) and after (b) stretching

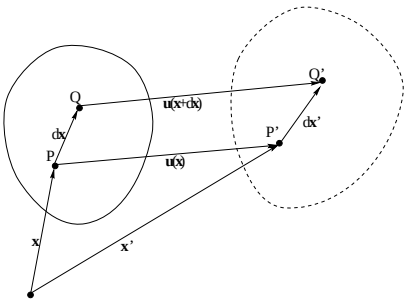

Figure 2: A body before and after deformation.

before and after deformation. The points P and Q undergo deformation such that they arrive in position $\mathbf{x}' = \mathbf{x} + \mathbf{u}(\mathbf{x})$ and $\mathbf{x}' + d\mathbf{x}' = \mathbf{x} + d\mathbf{x} + \mathbf{u}(\mathbf{x} + d\mathbf{x})$, respectively, where $\mathbf{u}$ is called the *displacement field*.

In order to understand the deformation we consider how two neighbouring points P and Q change in relation to each other. We have

$$d\mathbf{x}' = d\mathbf{x} + \mathbf{u}(\mathbf{x} + d\mathbf{x}) - \mathbf{u}(\mathbf{x})$$

which can be written as [4]

$$d\mathbf{x}' = d\mathbf{x} + (\nabla \mathbf{u}) d\mathbf{x}$$

where the second-order tensor

$$\nabla \mathbf{u} = \begin{pmatrix} \frac{\partial u_1}{\partial x_1} & \frac{\partial u_1}{\partial x_2} & \frac{\partial u_1}{\partial x_3} \\ \frac{\partial u_2}{\partial x_1} & \frac{\partial u_2}{\partial x_2} & \frac{\partial u_2}{\partial x_3} \\ \frac{\partial u_3}{\partial x_1} & \frac{\partial u_3}{\partial x_2} & \frac{\partial u_3}{\partial x_3} \end{pmatrix}$$

is known as the *displacement gradient*.

It can be seen that if $\nabla \mathbf{u} = 0$ then $d\mathbf{x}' = d\mathbf{x}$ and the motion in the neighbourhood of point P is that of a rigid body translation. The information about the material deformation around P is contained in $\nabla \mathbf{u}$. In order to define an entity which contains information about deformation without rigid body rotation consider two material vectors $d\mathbf{x}_1$ and $d\mathbf{x}_2$ issuing from point P. Their dot product can be shown to be ([4])

$$d\mathbf{x}_1'.d\mathbf{x}_2' = d\mathbf{x}_1.d\mathbf{x}_2 + 2d\mathbf{x}_1.\mathbf{E}^* d\mathbf{x}_2$$

where the symmetric second-order tensor

$$\mathbf{E}^* = \frac{1}{2}\left((\nabla \mathbf{u}) + (\nabla \mathbf{u})^T + (\nabla \mathbf{u})^T(\nabla \mathbf{u})\right)$$

is the *Lagrangian strain tensor*. Note that if $\mathbf{E}^* = 0$ the lengths and angles between the material vectors $d\mathbf{x}_1$ and $d\mathbf{x}_2$ remain unchanged, i.e., the deformation $\nabla \mathbf{u}$ around point P is an infinitesimal rigid body rotation. The components of $\mathbf{E}^*$ are

$$E^*_{ij} = \frac{1}{2}\left(\frac{\partial u_i}{\partial x_j} + \frac{\partial u_j}{\partial x_i} + \frac{\partial u_k}{\partial x_i}\frac{\partial u_k}{\partial x_j}\right)$$

For small deformations the displacement gradients $\partial u_i/\partial x_j$ are small and the quadratic term of $\mathbf{E}^*$ can be neglected giving the *strain tensor*

$$\epsilon_{ij} = \frac{1}{2}\left(\frac{\partial u_i}{\partial x_j} + \frac{\partial u_j}{\partial x_i}\right) \tag{2}$$

Lai et al. show [4] that for small values ϵ_{ii} can be interpreted as the unit elongation of a material element in the x_i direction and $2\epsilon_{ij}$, $i \neq j$ can be interpreted as the decrease in angle between two material vectors initially in the x_i and x_j directions.

Note that by definition the strain tensor $\boldsymbol{\epsilon}$ is symmetric. The eigenvectors $\mathbf{v}_1$, $\mathbf{v}_2$, and $\mathbf{v}_3$ of $\boldsymbol{\epsilon}$ are the *principal directions* of the strain, i.e., the directions where there is no shear strain. The eigenvalues λ_1, λ_2, and λ_3 are the *principal strains* and give the unit elongations in the principal directions. The maximum, medium, and minimum eigenvalue are called the *maximum, medium, and minimum principal strain*, respectively.

The meaning of the principal directions is illustrate in figure 3 which shows a body before (solid lines) and after (dashed lines) a deformation called *pure shear*. The eigenvectors of the corresponding strain tensor at any point are given by $\mathbf{v}_1$ and $\mathbf{v}_2$. It can be seen that the small square region axis-aligned with $\mathbf{v}_1$ and $\mathbf{v}_2$ is deformed into a rectangle, i.e., it does not experience a shear strain.

The importance of the shear strain is illustrated in figure 4 which shows two blocks of woods under a uniaxial load. The block in (a) has the wood fibers axis aligned with the direction of the load, whereas in (b) the wood fibers are aligned with the direction of the maximum shear strain given by the diagonal lines separating the blocks. It is intuitively clear that the block in (b) is more likely to fail under the applied load.

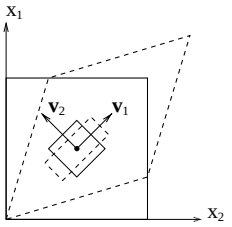

Figure 3: Principal stretch axes of a deformed body.

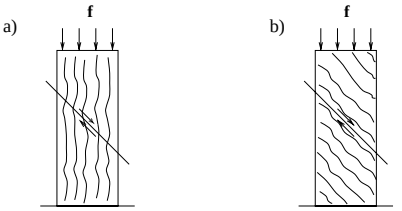

Figure 4: Shear strain in a block of wood.

4 Stress

The previous section gave a purely kinematical description of the motion and deformation of an elastic body without considering the internal and external forces causing it. Internal forces are body forces acting throughout the body (e.g., gravity) and external forces are surface forces acting on a real or imagined surface within the body. The surface force at a point of the surface is described by a *stress vector*.

Consider a plane S with normal $\mathbf{n}$ at a point P of the elastic body as shown in figure 5. Let $\Delta\mathbf{f}$ be the force acting on a small area ΔA containing P. The stress vector $\mathbf{t}_n$ at P is defined as

$$\mathbf{t}_n = \lim_{\Delta A \to 0} \frac{\Delta \mathbf{f}}{\Delta A}$$

In classical continuum theory the resulting stress vector is the same for all surfaces

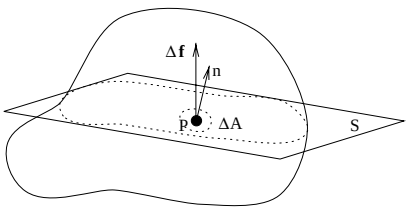

Figure 5: Definition of a stress vector.

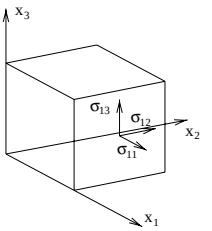

Figure 6: Stress components of a tensor.

through point P with a tangent plane S in P, i.e., it is independent of the surface curvature. It can be shown ([4]) that the stress vector acting on any plane with normal n through P can be expressed as

$$\mathbf{t}_n = \boldsymbol{\sigma}\mathbf{n}$$

where the linear operator $\boldsymbol{\sigma}$ defines the *stress tensor* in P.

To interpret the components of the stress tensor $\boldsymbol{\sigma}$ consider an infinitesimal small axis-aligned cube as shown in figure 6. The stress tensor components σ_{11}, σ_{12}, and σ_{13} are the components of the stress vector $\mathbf{t}_{\mathbf{e}_1}$. The other components of $\boldsymbol{\sigma}$ are

interpreted similarly. We call the diagonal elements σ_{11}, σ_{22}, and σ_{33} the *normal stresses* and the off-diagonal elements σ_{12}, σ_{13}, σ_{23}, σ_{21}, σ_{31}, and σ_{32} the *shear stresses*. By using the conservation of momentum equation it can be shown that $\boldsymbol{\sigma}$ is symmetric for most materials [4].

As for the strain tensor the three eigenvectors of the symmetric stress tensor $\boldsymbol{\sigma}$ give the *principal directions* of the stress. The eigenvalues of $\boldsymbol{\sigma}$ give the *principal stresses*. Each principal direction gives the normal direction of a plane on which the shear stresses are zero and the normal stress is the *principal stress*.

5 Visualization of Tensor Fields

The major sources of material failure in structural mechanics are stresses and strains. For an idealized isotropic and homogeneous material failure will occur if the maximum principal stress reaches a material dependent critical value. In practice complete knowledge of both the stress and the strain tensor fields is necessary to predict the material behaviour. For example, Aspden and Hukins [7, chapter 8] relate shear strains to fatigue syndromes in bone material whereas Rappitch et al. [3] compare wall shear patterns of the arterial wall with clinically observed disease patterns.

The difficulty of interpreting tensor data arises not only from the usually large size of the data sets but also from the fact that each tensor is represented by a matrix. The aim of tensor field visualization is therefore to transform these large amount of data into a single image which can be easily understood and interpreted by the user.

Two useful tools in visualizing data are *data transformation* and *data reduction*. Data transformation retains all the information in the data but presents it in a different form. As an example we have already presented the transformation of a tensor into its eigenvectors and eigenvalues. Data reduction on the other hand extracts only partial information from the original tensor data and so gives an incomplete representation. Examples of vector data obtained by reducing tensor data are principal stresses or strains together with the corresponding principal direction. Other useful vector data are the *surface traction vector* and the maximum shearing stress. Scalar data obtained by reducing tensor data includes: any principal stress or strain, the maximum shearing stress or strain, and the strain energy per unit volume [2].

6 Examples

In this section we explain several methods for tensor field visualization with the help of a standard problem in structural mechanics. We implemented a *Finite Element Method* modeller and various visualization algorithms to solve and visualize two and three-dimensional problems in linear elasticity. An an example we consider a plate with a hole under uniaxial load in y direction as shown in figure 7 (a). To make the resulting fields more interesting the plate is thickened around the hole. Because of symmetry we model only one quarter of the original plate (b).

A snapshot of our modelling and visualization toolkit is shown in figure 8. The model from figure 7 is shown in white solid lines and consists of 10 finite elements. For better results an automatic refinement algorithm can be applied before solving

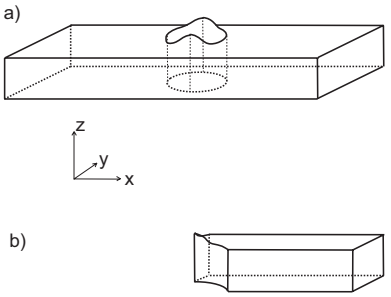

Figure 7: Plate with a hole.

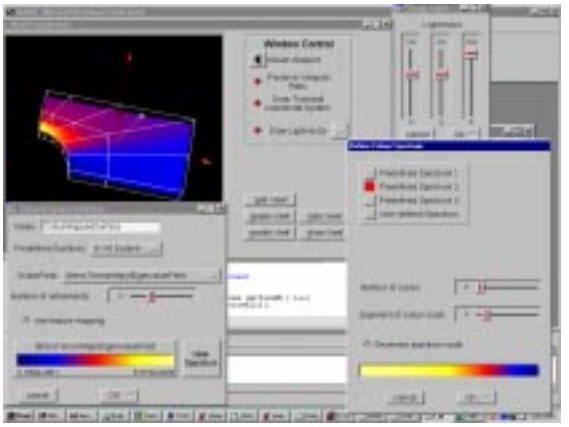

Figure 8: Snapshot of the tensor field visualization toolkit.

the FEM problem. Figure 8 visualizes the maximum principal stress on the surface bisecting the model in z-direction. The colour spectrum used interpolates piecewise linearly between white-yellow, saturated yellow, saturated red, saturated blue and blue-black. It is clearly visible that the maximum principal tensile stress on that surface occurs at the back of the hole. Note that the linear colour map used makes it very difficult to differentiate stress values and stress contours on the surface. An improvement is achieved in figure 9 by defining a cyclical colour map and mapping the scalar data over eight colour cycles.

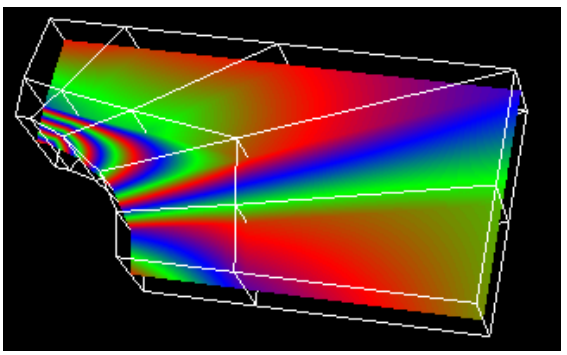

Figure 9: Maximum principal stress visualized with a cyclical colour map.

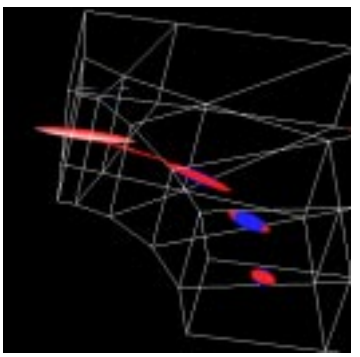

Figure 10: Tensor ellipsoids.

In order to evaluate the impact of an applied load knowledge of the stress direction is important. The full tensor information at discrete points is given by *tensor ellipsoids* shown in figure 10. The directions and lengths of the principal axes of a tensor ellipsoid are given by the eigenvectors and eigenvalues of the tensor, respectively. We additionally visualize the sign of each eigenvalue by using blue for a negative value (compressive stress) and red for a positive value (tensile stress). Figure 10 shows that the tensile stress at the back of the hole is tangential to the

hole surface. Together with the information obtained by the colour mapped surface we can therefore conclude that the plate will most likely fail at the back of the hole.

Using many tensor ellipsoids close together leads to visual cluttering. This problem can be prevented by using *hyperstreamlines* [1] which contain the full tensor information along a continuous line. The trajectory of a hyperstreamline is an integral curve $\mathbf{x}(s)$ satisfying

$$\frac{d\mathbf{x}}{ds} = \mathbf{v}(\mathbf{x}) \tag{3}$$

where $\mathbf{v}$ is one of the eigenvector fields of the tensor field. The other two eigenvectors and corresponding eigenvalues define the axes and length of the ellipsoidal cross section of the hyperstreamline. The eigenvalue corresponding to the eigenvector defining the trajectory is colour mapped onto the surface of the hyperstreamline. An example is given in figure 11. The narrowing in the hyperstreamline indicates the area where the medium principal stress switches sign.

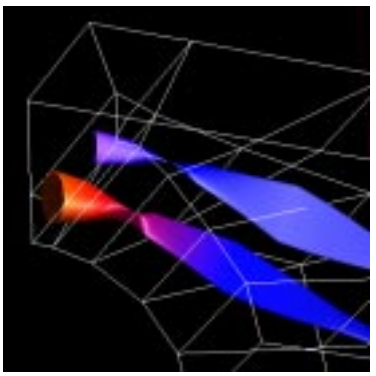

Figure 11: Stress field visualized by two hyperstreamlines.

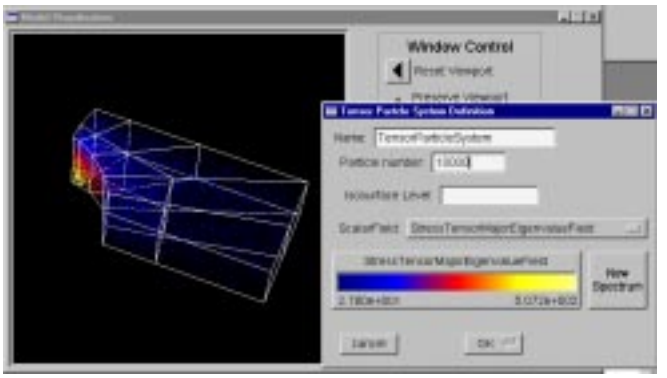

Figure 12: Tensor particles visualizing the maximum principal stress.

As a new visualization method we present tensor particles. Distributing the particles randomly over the domain gives a good impression of the stress field. Particles can be colour coded by any of the principal stresses or any other derived entity. Using tensor particles figure 12 reveals that the maximum tensile stress occurs at the bottom of the back of the hole. The plate will therefore most likely crack in that area. Moving the particles along the gradient of a principal stress field and constraining them to user defined isovalues defines isosurfaces. An example is given in figure 13. At the moment we are implementing interactive methods to expand selected particles into tensor ellipsoids or, by tracing, into tensor streamlines and hyperstreamline.

7 Conclusion

We have presented a simple introduction to stress and strain fields as they occur in elastic bodies. An understanding of the stresses and strains in a body is important in engineering, medicine, and biomechanics since they are the major source of material failure and are necessary for the understanding of organ function [2].

Interpreting large amounts of tensor data is difficult, though, since a tensor is equiv-

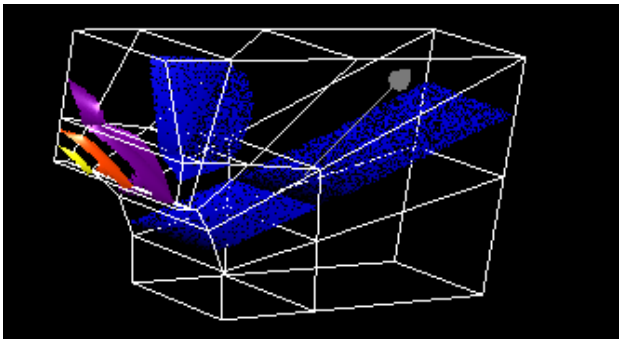

Figure 13: Systems of illuminated and oriented particles visualizing isosurfaces.

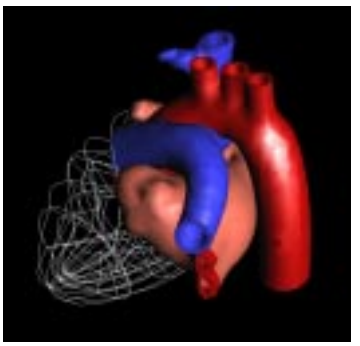

Figure 14: The heart model.

alent to a matrix. As a solution we have presented several old visualization methods for tensor fields, and one new one.

Our work was motivated by the Bioengineering Research Group of the University of Auckland which uses a combination of mathematical modeling and experimental results to construct a model of a canine heart (fig 14). We are currently extending our FEM modeller and visualization toolkit to deal with the tricubic elements used in the model. Visualizing the stress and strain fields in the heart can be used for diagnosis, surgical planning, and the evaluation of the success of surgery.

References

[1] Thierry Delmarcelle and Lambertus Hesselink. Visualizing second order tensor fields with hyperstreamlines. *IEEE Computer Graphics and Applications*, 13(4):25 – 33, 1993.

[2] Y. C. Fung. *Biomechanics - Motion, Flow, Stress, and Growth*. Springer Verlag New York Inc., 1990.

[3] K. D. Held, C. A. Brebbia, R. D. CisKowski, and H. Power, editors. *Computational Biomedicine*. Computational Mechanics Publications, Ashurst, Southampton SO4 2AA, UK, 1993.

[4] W. Michael Lai, David Rubin, and Erhard Krempl. *Introduction to Continuum Mechanics*. Pergamon Press, Oxford, 1986.

[5] Frederic I. Parke and Keith Waters. *Computer Facial Animation*. A K Peters Ltd., Wellesley, Massachusetts, 1996.

[6] Mark A. Sagar, David Bullivant, Gordon D. Mallinson, Peter J. Hunter, and Ian W. Hunter. A virtual environment and model of the eye for surgical simulation. In Andrew Glassner, editor, *Proceedings of SIGGRAPH '94*, pages 205–213, July 1994.

[7] A. L. Yettram, editor. *Material properties and stress analysis in biomechanics*. Manchester University Press, 1989.